Synergy of Eed and Tsix in the repression of Xist gene and X-chromosome inactivation

[Title page]

Synergy of Eed and *Tsix* in the repression of *Xist* gene and X-chromosome inactivation (84 characters)

Shinwa Shibata[1]*, Takashi Yokota[1], and Anton Wutz[2]

[1]Department of Stem Cell Biology, Graduate School of Medicine, Kanazawa University, 13-1 Takara-machi, Kanazawa, Ishikawa 920-8640, Japan

[2]Research Institute of Molecular Pathology, 1030 Vienna, Austria

*To whom correspondence should be addressed:

Shinwa Shibata Tel: +81-76-265-2208; Fax +81-76-234-4238;

E-mail: shinwa@med.kanazawa-u.ac.jp

The total character count of the manuscript is: 50,223.

Running title: Synergy of Eed and *Tsix* in *Xist* repression (42 characters)

Abstract

X-chromosome inactivation (XCI) depends on the noncoding *Xist* gene. *Xist* transcription is negatively regulated by its antisense partner *Tsix*, whose disruption results in non-random XCI in females. However, males can maintain *Xist* in a repressed state without *Tsix*, indicating participation of additional factor(s) in the protection of the single male X from inactivation. Here we provide evidence that the histone methyltransferase Eed is also involved in the process. Male embryonic stem cells with *Eed*-null and *Tsix* mutations ($X^{\Delta}Y$ *Eed-/-*) showed *Xist* hyperactivation upon differentiation, while cells with either mutation alone did not. Impaired X-linked gene expression was observed in the $X^{\Delta}Y$ *Eed-/-* ES cells at the onset of differentiation. The *Xist* promoter in the $X^{\Delta}Y$ *Eed-/-* cells showed elevated histone H3-dimethyl lysine 4 modifications and lowered CpG methylation, which are characteristic of open chromatin. Hence, we identified Eed as an additional major player in the regulation of *Xist* expression. The synergy of Polycomb group proteins and antisense *Tsix* transcription in *Xist* gene regulation explains why males can repress *Xist* without *Tsix*. (171 words)

Subject Category: Chromatin & Transcription

Keywords: antisense / DNA methylation / Eed / histone modification / *Xist*

Introduction

X-chromosome inactivation (XCI) is a sex chromosome dosage compensation mechanism employed by female mammals. During the process, one of two active X-chromosomes (Xa) in female embryonic cells is randomly chosen and inactivated during development (Lyon, 1961; reviewed by Heard and Disteche, 2006). The noncoding gene *Xist* (Brockdorff *et al*, 1992; Brown *et al*, 1992) has been shown to be critical for XCI (Penny *et al*, 1996). It is encoded on the X-chromosome and is transcribed at a very low level in the undifferentiated condition in both females and males (Panning and Jaenisch, 1996; Lee *et al*, 1999). Upon differentiation it is exclusively expressed from the inactive X-chromosome (Xi) and coats Xi in females (Clemson *et al*, 1996), while *Xist* transcription is soon terminated on the future Xa and in males. The choice of Xi is achieved by *Xist* upregulation in *cis* (Wutz and Jaenisch, 2000). *Xist* is believed to function as an RNA entity, because of its characteristic repeat sequence (Wutz *et al*, 2002) and distribution pattern in the nucleus. *Xist* is negatively regulated by its antisense partner *Tsix*, which overlaps the *Xist* gene (Lee *et al*, 1999; Sado *et al*, 2001; Shibata and Lee, 2003). *Xist* is always upregulated at the mutant *Tsix* allele in heterozygous female embryonic stem (ES) cells, resulting in non-random inactivation of the *Tsix* mutated X (Lee and Lu, 1999; Sado *et al*, 2001; Luikenhuis *et al*, 2001; Shibata and Lee, 2004). In contrast, *Tsix* mutation does not lead to *Xist* expression in male ES cells upon differentiation. Previous reports described ectopic *Xist* accumulation in a minor portion of *Tsix* mutant male ES cells (0-13%) (Lee and Lu, 1999; Luikenhuis *et al*, 2001; Sado *et al*, 2002), while another study observed ectopic *Xist* accumulation more frequently (39%) (Vigneau *et al*, 2006). Importantly, male embryos carrying a *Tsix* mutation on the single X develop to term when the

extraembryonic tissues are complemented by wild-type tetraploid cells (Ohhata *et al*, 2006), indicating that most embryonic cells in males can maintain *Xist* gene repression without *Tsix*. These observations suggest the presence of additional or alternative factor(s) that inhibit the activation of *Xist* gene in male embryos.

Recent studies have shed light on the role of *Tsix* in regulating chromatin structure in the *Xist* locus. Sado *et al* indicated that disruption of *Tsix* caused impaired establishment of repressive chromatin structure at the *Xist* promoter and exon 1 in developing embryos (Sado *et al*, 2005). Navarro *et al* showed that the *Xist* promoter region, flanked by CTCF-binding sites, was maintained in a heterochromatic state by *Tsix*. *Tsix* truncation resulted in altered modification at lysine 4 of histone H3 (H3K4) and -lysine 9 to resemble a pseudoeuchromatic state (Navarro *et al*, 2006). Sun *et al* reported that *Tsix* downregulation induced a transient heterochromatic state, characterized by histone H3 trimethyl-lysine 27 (H3K27m3) modification in undifferentiated female ES cells (Sun *et al*, 2006). These reports suggest that *Tsix* transcription influences the chromatin structure at the *Xist* promoter in different ways depending on the differentiation stage and position within the locus. We focused on H3K27m3, because this modification is clearly elevated when *Tsix* transcription is absent in both female and male undifferentiated ES cells (Navarro *et al*, 2006; Sun *et al*, 2006; Shibata and Yokota, 2008). In addition, the biological significance of the regulation by *Tsix* of the H3K27m3 modification is still unclear. The H3K27m3 modification is generally considered to be a repressive chromatin mark, however, the loss of *Tsix* transcription paradoxically results in *Xist* gene activation in females.

Methylation of the histone H3 lysine 27 (H3K27) is conferred by the Polycomb repressive complex 2 (PRC2) that is composed of the Eed, Ezh2, and Suz12 proteins

(Cao and Zhang, 2004). Eed is essential for the histone methyltransferase (HMTase) activity, because *Eed*-/- ES cells lack the H3K27m3 modification (Montgomery *et al*, 2005). Eed is necessary for development (Faust *et al*, 1995) and regulates developmental control genes as well as a subset of imprinted genes (Mager *et al*, 2003). In ES cells, PRC2 occupies genes encoding transcription factors crucial for development, and *Eed* mutations result in their premature expression (Boyer *et al*, 2006; Azuara *et al*, 2006). These loci were termed bivalent domains due to the special modification pattern consisting of trimethylated H3K27 and H3K4, a repressive and active chromatin mark, respectively (Bernstein *et al*, 2006). Hence, Eed plays a role in gene regulation in undifferentiated and differentiating cells in conjunction with other chromatin factors. Eed and H3K27 methylation are also involved in establishment and maintenance of XCI. Eed localizes on the Xi in female trophoblast stem cells and reactivation of Xi is found in *Eed*-/- trophoblast stem cells when they are differentiated (Kalantry *et al*, 2006). Recruitment of Eed and H3K27 methylation are also observed on Xi in female embryos and ES cells at early stages of XCI (Plath *et al*, 2003; Silva *et al*, 2003). However, recent findings indicate that Eed is dispensable for the initiation of random XCI (Schoeftner *et al*, 2006; Kalantry and Magnuson, 2006). XCI without Eed is explained by a contribution of Polycomb repressive complex 1 (PRC1) that ubiquitinates histone H2A (Schoeftner *et al*, 2006). These reports focused mainly on the role of Eed in inducing global heterochromatin formation on Xi, but as was shown by Sun *et al*, Eed is likely to have additional roles in the regulation of local *Xist* chromatin structure in concert with *Tsix*. Therefore, we disrupted *Tsix* in an *Eed*-/- male ES cell line to investigate the role of Eed in regulating *Xist* chromatin structure and to examine the biological significance of the H3K27m3 modification that is observed when *Tsix*

transcription is absent. The role and relationship of Eed and *Tsix* in the regulation of *Xist* are discussed.

Results

Generation of male Tsix mutant ES cells with Eed-/- background

Tsix mutant ES cell lines are summarized in Figure 1A. Firstly, we targeted the clone36 *Eed-/-* male ES cell line (XY *Eed-/-*) (Schoeftner *et al*, 2006) and truncated *Tsix* transcription to generate male *Tsix* mutant ES cells with an *Eed-/-* background ($X^{\Delta}Y$ *Eed-/-*) (Figure 1B-D). This type of *Tsix* mutation has been shown to eradicate its function in repressing *Xist* in female ES cells ($X^{\Delta}X$) (Shibata and Lee, 2004). We then rescued Eed in the XY *Eed-/-* and $X^{\Delta}Y$ *Eed-/-* cells by transgenic expression of an EGFP (enhanced green fluorescent protein)-Eed fusion protein (XY *Eed-TG* and $X^{\Delta}Y$ *Eed-TG*, respectively) (Figure 1E and F). In addition to the western blot for H3K27m3, a quantitative chromatin immunoprecipitation (ChIP) assay was used to examine known H3K27m3-labelled sites in undifferentiated ES cells, the *Sox9* and *Gata6* promoters (Boyer *et al*, 2006), and confirmed that the Eed activity was sufficiently rescued in the $X^{\Delta}Y$ *Eed-TG* cells for these promoters (Supplementary Figure S1). Although the clone36 *Eed-/-* ES cells have an additional *Xist* cDNA transgene (Tg) under control of tetracycline-inducible promoter on chromosome 11, the *Xist* Tg has been shown to be inactive without induction (Wutz and Jaenisch, 2000).

$X^{\Delta}Y$ Eed-/- cells display Xist hyperactivation upon differentiation

We examined *Xist* RNA expression in the $X^{\Delta}Y$ *Eed-/-* cells by fluorescent *in situ* hybridization (FISH) using a strand-specific riboprobe. We found strong *Xist* expression in the $X^{\Delta}Y$ *Eed-/-* cells, but not in the XY *Eed-/-* embryoid bodies (EB) differentiated for 3 days (Figure 2A and B). The number of *Xist*-positive nuclei was found significantly elevated in two independent $X^{\Delta}Y$ *Eed-/-* lines, and was similar to that of

differentiating $X^{\Delta}X$ ES cells (Figure 2C and Supplementary Table I). Polymorphism of an *Xist* RT-PCR product confirmed that the ectopic *Xist* expression in the $X^{\Delta}Y$ *Eed-/-* EB was from the endogenous *Xist* allele, not from the *Xist* cDNA Tg, which is also present in all clone36 derived ES cells (Figure 2D). The amount of *Xist* RNA expressed during the course of XCI was further quantified by real-time PCR. The results were normalized to *Gapdh (glyceraldehyde-3-phosphate dehydrogenase)* expression and the amount of *Xist* RNA expression, relative to undifferentiated wild-type female (XX) ES cells, is shown (Figure 2E and Supplementary Table II). Interestingly, the $X^{\Delta}Y$ *Eed-/-* ES cells showed elevated *Xist* RNA level even in the undifferentiated condition, and upon differentiation they expressed five to ten times more *Xist* RNA than XX cells. The XY *Eed-/-* EB also displayed elevated *Xist* level when compared to undifferentiated XY *Eed-TG* cells, but far less than XX and $X^{\Delta}Y$ *Eed-/-* EB. We then investigated whether the loss of Eed was the cause of this result, because *Xist* activation does not generally occur in male *Tsix* mutant ES cells. We looked for suppression of ectopic *Xist* hyperactivation in the $X^{\Delta}Y$ *Eed-TG* cells and confirmed that the rescued Eed successfully inhibited *Xist* hyperactivation (Figure 2F). Therefore, both *Tsix* and Eed contribute to the repression of *Xist* gene, but either of the two is sufficient for preventing ectopic *Xist* activation in males.

Xist hyperactivation in the $X^{\Delta}Y$ Eed-/- cells leads to partial XCI upon differentiation

We next investigated the consequence of *Xist* hyperactivation in the $X^{\Delta}Y$ *Eed-/-* cells by differentiating the mutant ES cells in vitro. The $X^{\Delta}Y$ *Eed-/-* ES cells in the undifferentiated condition displayed round, well-packed colony morphology typical of mouse ES cells (Figure 3A). The $X^{\Delta}Y$ *Eed-/-* EB cells, after long adherent culture,

contained flattened cells suggesting differentiation (Figure 3B), but it was not clear whether their X-chromosomes were inactivated or not. The growth of XY *Eed-/-* EB cells were retarded as compared to the EB cells with intact Eed (Figure 3C). Expression of transgenic Eed rescued their poor growth (Supplementary Figure S2). The growth of $X^{\Delta}Y$ *Eed-/-* EB cells was further retarded compared to the XY *Eed-/-* EB cells: they spread less and their EB size was smaller than that of the XY *Eed-/-* EB cells (Figure 3C and Supplementary Figure S2). This observation suggested that a substantial amount of differentiating $X^{\Delta}Y$ *Eed-/-* cells were lost from culture due to the inactivation of their single X-chromosome. To examine if XCI occurs in the $X^{\Delta}Y$ *Eed-/-* cells during differentiation, we studied the expression of X-linked *Mecp2*, *Pgk1*, and *Chic1* genes by quantitative RT-PCR (qRT-PCR) (Figure 3D). The expression of these genes decreased immediately upon differentiation, and interestingly, the reduction became less obvious at the late stage of EB day 12. We also examined co-localization of the Xi chromatin marker, histone H4 monomethyl-lysine 20 (H4K20m1) (Kohlmaier *et al,* 2004) with *Xist* RNA in immuno-FISH. Although *Xist* RNA deposition was frequently found in the $X^{\Delta}Y$ *Eed-/-* EB nuclei, co-localization of *Xist* and condensed H4K20m1 was never detected in the late stages of differentiation in contrast to the $X^{\Delta}X$ nuclei (Figure 3E and Table I). Careful examination of EB cells at day 2 or 4 revealed weak H4K20m1 staining with *Xist* paint in a maximum of 10% of the $X^{\Delta}Y$ *Eed-/-* nuclei (Supplementary Figure S3 and Supplementary Table III). Taken together, these findings indicate that the *Xist* hyperactivation in the $X^{\Delta}Y$ *Eed-/-* cells induced partical XCI at the onset of differentiation. However, it was incomplete, presumably due to the absence of Eed, and a substantial number of cells survived and restored their X-linked gene expression after the critical time window for silencing by *Xist* RNA (Wutz and Jaenisch, 2000)

(Supplementary Figure S4).

Deregulated antisense transcription in the Xist gene body of the X$^{\Delta}$Y Eed-/- ES cells

We confirmed that *Tsix* transcription was successfully truncated in the X$^{\Delta}$Y *Eed-/-* ES cells by a northern blot of poly-A purified RNA, using a probe residing in the *Xist* promoter (Figure 4A and B). However, antisense RNA was detected in the double mutant cells by strand-specific RT-PCR, and it disappeared when Eed was rescued (Figure 4C). In order to eliminate the possibility that the transcript originated from the *Xist* cDNA Tg, we performed qRT-PCR for *Tsix* in amplicons that do not amplify the Tg (Figure 4D). The amplicon at the 3'-end of the *Tsix* (#4) antisense transcript was not detected in the X$^{\Delta}$Y *Eed-/-* cells, whereas in the amplicon spanning the *Xist* introns (#5) could be detected. We suggest that the loss of Eed in the *Tsix*-deficient background resulted in an open chromatin structure that led to deregulated antisense transcription from cryptic promoters to various degrees in the *Xist* gene body. The absence of an antisense transcript at the 3'-end of *Tsix* suggested that the transcript was terminated by multiple poly-A signals in the antisense orientation residing near the *Xist* transcription start site (Shibata and Lee, 2003). Average *Tsix* expression levels observed by qRT-PCR were lower in the XY *Eed-/-* and XY *Eed-TG* lines than the wild-type male ES cells, but the difference was not statistically significant.

The X$^{\Delta}$Y Eed-/- ES cells display loss of CpG methylation at the Xist promoter

DNA in the *Xist* locus has been shown to be methylated in undifferentiated male ES cells (Norris *et al*, 1994). We examined the methylation level of the *Xist* locus in undifferentiated X$^{\Delta}$Y *Eed-/-* ES cells by Southern blot using methylation-sensitive

restriction enzymes. The *Sac*II site at the *Xist* promoter displayed lowered CpG methylation in the $X^{\Delta}Y$ *Eed-/-* cells (Figure 5A). This was also the case in the *Hpa*II site within *Xist* exon 1, which was revealed by comparing the intensity of methylated bands (Figure 5B). Note that the unmethylated band in Figure 5B represents both endogenous *Xist* and *Xist* cDNA Tg. Extra bands observed in Figure 5B originated from the *Xist* cDNA Tg, which was obvious to identify due to the absence of an *Eco*RI site and the presence of multiple *Hpa*II sites in the tetracycline inducible promoter and its flanking sequence. Rescuing Eed in the $X^{\Delta}Y$ *Eed-/-* cells ($X^{\Delta}Y$ *Eed-TG*) resulted in partial reversion of CpG methylation, which is in contrast to the previous report which showed a *Tsix* mutation did not affect the methylation status of *Xist* locus in males (Sun *et al*, 2006). Given that the *Xist* locus in the $X^{\Delta}Y$ *Eed-/-* ES cells takes an open chromatin configuration, as was shown by reduced CpG methylation and *Xist* hyperactivation upon differentiation, we suggest that once opened, the chromatin can not easily reset to a repressed condition by rescuing Eed activity.

The $X^{\Delta}Y$ Eed-/- ES cells display elevated H3K4 methylation at the Xist promoter

In order to gain further insight into the role of Eed and *Tsix* in *Xist* chromatin structure regulation, we examined the methylation of H3K4 and H3K27, and recruitment of transcription factor IIB (TFIIB) by the ChIP assay. Here it must be considered again that the XY *Eed-/-* cells and their derivatives contain an *Xist* cDNA Tg that includes *Xist*-GB1 and *Xist*-GB2 amplicons, but not others (Figure 6A). The H3K27m3 modification was no longer found in the $X^{\Delta}Y$ *Eed-/-* cells, confirming that Eed is responsible for the modification that appears when *Tsix* is absent (Figure 6B). Rescuing Eed resulted in a clearly elevated H3K27m3 level at the *Xist* promoter (*Xist*-P) in the

$X^{\Delta}Y$ *Eed-TG* cells ($p<0.0005$). PRC1 and its product monoubiquitinated histone H2A (UbH2A) are linked to Xi (de Napoles *et al*, 2004; Schoeftner *et al*, 2006), and they contribute to the control of developmental regulator genes (Stock *et al*, 2007). We examined if UbH2A modification at the *Xist* promoter is affected by *Tsix* mutations in both *Eed*+/+ and -/- cell lines (Supplementary Figure S5). In all cases the modification was nearly to the background level and we did not detect a statistically significant difference between the wild-type and *Tsix*-deficient lines. The loss of *Tsix* in the *Eed-/-* background resulted in a significantly increased dimethyl-H3K4 (H3K4m2) level at the *Xist* promoter and gene body (*Xist*-GB1). Both of these amplicons are within the previously reported CTCF-flanked region, and the level of H3K4m2 was comparable to that in the report (Navarro *et al*, 2006) (Figure 6C). Such augmented H3K4m2 level in the $X^{\Delta}Y$ *Eed-/-* cells was not clear outside of the CTCF-flanked region (*Xist*-GB2) or at 5'-portion of *Tsix* (5'-*Tsix*). We also found significantly elevated TFIIB recruitment at the *Xist* promoter in the $X^{\Delta}Y$ *Eed-/-* cells (Figure 6D), though it might be just reflecting the large transcription difference of *Xist* gene. Upon differentiation the H3K4m2 level at the *Xist* promoter persisted to be higher in the $X^{\Delta}Y$ *Eed-/-* EB than in XY *Eed-/-* EB. Enhanced H3K4m2 levels are consistent with the observed *Xist* hyperactivation (Figure 6E). Because the H3K4m2 modification in the *Xist* locus disappears upon differentiation in both wild-type and *Tsix* mutant male ES cells (Shibata and Yokota, 2008), we conclude that the *Tsix* mutation in the absence of Eed resulted in persistent high H3K4m2 level around the *Xist* promoter.

Tsix and Eed have a synergistic role in repressing Xist

Taken together with data from ChIP, RT-PCR, and CpG methylation analyses, we

present a summary illustrating the roles of *Tsix* and Eed in the regulation of *Xist* chromatin structure (Figure 7). *Xist* chromatin is most condensed in the $X^{\Delta}Y$ (or $X^{\Delta}Y$ *Eed-TG*) ES cells, followed by XY (or XY *Eed-TG*) and XY *Eed-/-* cells, and becomes highly opened in the $X^{\Delta}Y$ *Eed-/-* ES cells. The opened *Xist* chromatin configuration in the $X^{\Delta}Y$ *Eed-/-* ES cells allows *Xist* hyperactivation upon differentiation. These results suggest a model that *Tsix* transcription negatively regulates both PRC2 and H3K4 HMTase at the *Xist* promoter and exon 1. It has been shown that *Tsix* transcription prevents Eed/PRC2 recruitment to the *Xist* promoter in *cis* (Sun *et al*, 2006). *Tsix* transcription has also been reported to inhibit H3K4 methylation (Navarro *et al*, 2006), whereas the difference in H3K4m2 levels between the XY *Eed-TG* and $X^{\Delta}Y$ *Eed-TG* cells was not prominent (Figure 6C). The increased PRC2 recruitment or elevated H3K27m3 modification may inhibit H3K4 HMTase localization or the activity at the *Tsix*-deficient allele. The loss of Eed alone does not result in highly opened chromatin because *Tsix* still inhibits H3K4 HMTase. When both *Tsix* and Eed are absent, augmented H3K4 HMTase activity confers highly elevated H3K4 methylation that induces ectopic *Xist* activation upon differentiation. The mechanism of *Xist* hyperactivation in the $X^{\Delta}Y$ *Eed-/-* cells is in clear contrast to that of the physiological *Xist* activation in female future Xi. In the latter, *Xist* RNA yield is limited, and in females *Xist* transcription is activated at *Tsix*-deficient alleles with elevated H3K27m3 modification (Sun *et al*, 2006). Hence, we suggest that Eed contributes in male cells to inhibit ectopic *Xist* activation during differentiation when *Tsix* transcription goes down.

Discussion

Inability of the X$^{\Delta}$Y Eed-/- ES cells to repress Xist despite of intact counting

We demonstrated that the male ES cells with both *Eed*-null and *Tsix* mutations underwent ectopic *Xist* hyperactivation upon differentiation. This result can be attributed to either defective X-chromosome counting or dysfunction in *Xist* gene regulation. The *Tsix* mutant allele generated in this study does not lose any DNA elements necessary for X-chromosome counting, because the female ES cells heterozygous for the mutation did not show aberrant counting such as two Xi or no Xi (Shibata and Lee, 2004). The counting function has been ascribed to *Xite* (Ogawa and Lee, 2003) and an additional region at the 5'-portion of *Tsix* (Morey *et al*, 2004; Lee, 2005). Both DNA elements are completely conserved in the X$^{\Delta}$Y *Eed-/-* cells, and they are not included in the *Xist* cDNA Tg. Similarly, the DNA elements required for homologous chromosome pairing at the onset of XCI (Bacher *et al*, 2006; Xu *et al*, 2006) are retained in the X$^{\Delta}$Y *Eed-/-* cells and are not involved in the Tg. Thus, we conclude that the X$^{\Delta}$Y *Eed-/-* cells have a dysfunction in *Xist* regulation, *i.e.* the mutant male ES cells are unable to repress *Xist* upon differentiation. It has long been unexplained why and how male ES cells can repress *Xist* without *Tsix*, although it is critical in females. Our findings demonstrated a synergistic role of *Tsix* and Eed in *Xist* regulation and indicated that Eed alone could effectively block ectopic *Xist* activation. In this context, our observation that the X$^{\Delta}$Y *Eed-/-* cells accumulated much more *Xist* RNA than wild-type female cells upon differentiation is reasonable, because the mutant cells have lost control of *Xist* transcription. We have identified Eed as an additional major player in regulating *Xist* expression and in the protection of future Xa from ectopic inactivation, this being the conceptual advance provided by this report.

Ectopic Xist activation in the $X^{\Delta}Y$ Eed-/- cells depends on a different mechanism from physiological Xist activation in females

We suggest that the open chromatin structure at the *Xist* promoter and exon 1 in the $X^{\Delta}Y$ *Eed-/-* cells resulted in ectopic *Xist* hyperactivation, presumably by transcription factors which are not included in the physiological *Xist* transcription in females. It is also possible that some factors with *Xist* activator function are derepressed in *Eed*-null males and caused *Xist* activation in the $X^{\Delta}Y$ *Eed-/-* cells, because many developmental regulators are prematurely activated in *Eed*-null ES cells (Boyer *et al*, 2006; Azuara *et al*, 2006). In undifferentiated male ES cells, the loss of Eed resulted in a 4.6 times increment in the *Xist* RNA level (Supplementary Table II, XY *Eed-TG* vs. XY *Eed-/-*) whereas the loss of *Tsix* results in only a 1.6 times increment (Sun *et al*, 2006). In addition the XY *Eed-/-* cells consistently showed an elevated *Xist* RNA level during differentiation. Therefore, Eed makes a substantial contribution in repressing *Xist* even in the presence of *Tsix*. Intriguingly, female ES cells heterozygous for a *Tsix* mutation can activate *Xist* transcription at the mutant allele despite the presence of H3K27m3 modification at the promoter (Sun *et al*, 2006). Hence, unlike non-specific *Xist* activation, the physiological transcription factor for *Xist* can work if the promoter is H3K27-methylated. The transcription factor involved in *Xist* activation has not been discovered yet, and identification of the factor would be beneficial in understanding the regulation of XCI.

Eed and Tsix have synergistic, but autonomous functions in Xist regulation

Previous reports have shown that, in the absence of *Tsix* transcription, both active

chromatin marker H3K4m2 and repressive marker H3K27m3 increase at the *Xist* promoter (Navarro *et al*, 2006; Sun *et al*, 2006; Shibata and Yokota, 2008), suggesting that *Tsix* inhibits H3K4 HMTase and PRC2 activity, together. Though we need further study in order to look into the molecular mechanism, it is likely that antisense transcription has a role in stabilizing local chromatin structure by preventing additional histone modifications. This hypothesis is strengthened by previous observations that the *Xist* locus in male ES cells is already in a repressed state in terms of CpG methylation (Norris *et al*, 1994; Sun *et al*, 2006) that is required for stable *Xist* repression (Panning and Jaenisch, 1996; Barr *et al*, 2007). We suggest that in undifferentiated female cells, prolonged *Tsix* transcription on the future Xa prevents the reorganization of repressive *Xist* chromatin structure while immediate *Tsix* shut down on the future Xi allows conversion to an active state, resulting in transcriptional activation of *Xist*. Importantly, *Tsix* transcription can also regulate *Xist* in an Eed-independent manner because the *Xist* is not hyperactivated in XY *Eed-/-* cells. It is still not clear whether the Eed-independent *Xist* regulation by *Tsix* is solely based on the inhibition of H3K4 methylation, or if there is an additional molecular mechanism other than histone modifications. Trithorax group proteins are known to antagonize Polycomb group proteins, and human Trithorax group proteins MLL and ASH1L have been shown to have H3K4 HMTase activity (Milne *et al*, 2002; Gregory *et al*, 2007). The di- and trimethyl H3K27 demethylase UTX was reported to associate with MLL complexes and induce H3K4 methylation at the promoters of *HOX* genes (Lee *et al*, 2007). Most intriguingly, *Drosophila* UTX co-localizes with RNA polymerase II (Smith *et al*, 2008), implying possible association of UTX with *Tsix* transcription in the regulation of H3K27m3 modification in the *Xist* locus. We anticipate studies on the involvement of these HMTases and histone

demethylases in the control of XCI.

Antisense RNA in the Xist gene body cannot prevent Xist activation

There is also an issue as to whether *Tsix* functions as an RNA entity or if transcription itself is sufficient. At present there is no evidence showing that *Tsix* works as an RNA molecule (Shibata and Lee, 2004; Sado *et al*, 2006). Our finding that *Xist* could not be repressed despite the deregulated antisense transcription in the $X^{\Delta}Y$ *Eed-/-* cells sheds some light on this issue. One possible interpretation is that continual *Tsix* transcription over the entire 40 kb length is necessary in order to organize the local chromatin structure and/or to retain proper subnuclear localization of the locus. Recent transcriptome analysis indicated that paired sense/antisense expression is not restricted to imprinted loci, and that overlapping transcript pairs are more widespread in the mammalian genome than was thought previously (Katayama *et al*, 2005). Various types of interactions between the pairs are suggested, and at least some of them are likely to work through chromatin. Studies on the molecular mechanism of *Tsix*'s action in repressing *Xist* would provide useful hints for understanding the function of antisense genes.

Materials and Methods

Targeting construct

The pBl/E7EBS plasmid having a 6.7 kb *Eco*RI-*Bam*HI fragment of *Xist* exon 7 followed by a 3.0 kb fragment of the *Xist* 3'-end (Shibata and Lee, 2004) was digested by *Bam*HI, blunted-ended, and ligated with *Sal*I-digested and blunted-ended 3.6 kb SA.IRES.hygro.pA2 fragment from pGT1.8IREShygropA2 (Nichols *et al*, 1998), yielding the targeting vector pBl/E7EBS/SIHA.

Cell culture and generation of cell lines

Clone 36 *Eed-/-* male ES cells (XY *Eed-/-*) were electroporated with *Sal*I-linearized pBl/E7EBS/SIHA vector and selected as described (Schoeftner *et al*, 2006) to generate $X^{\Delta}Y$ *Eed-/-* lines. Colonies were screened as reported (Shibata and Lee, 2004; Shibata and Yokota, 2008). The EL16.7 female ES cell (XX), EL16.7-derived *Tsix*-trap cell ($X^{\Delta}X$) (Shibata and Lee, 2004), E14.1 male ES cell (XY), and E14.1-derived *Tsix*-trap cell ($X^{\Delta}Y$) (Shibata and Yokota, 2008) were used as controls. The J1 male ES cell line was used for EB formation in Supplementary Figure S1 and H3K27m3 ChIP assay in Supplementary Figure S2. Generation of the XY *Eed-TG* lines was as described (Schoeftner *et al*, 2006). For generation of the $X^{\Delta}Y$ *Eed-TG* lines, the $X^{\Delta}Y$ *Eed-/-* cells were electroporated with 50 μg of pCAG-EGFP-Eed-IREShyg-PA plasmid and cultured in the presence of 260 μg/ml of hygromycin. When cells became confluent, they were trypsinized and GFP-positive cells were sorted using a JSAN cell sorter (Bay bioscience, Kobe, Japan), replated, and grown until the next cell sorting. After three rounds of sorting enrichment, cells were split and GPF-positive single colonies were selected under a fluorescent microscope and isolated. For EB formation, trypsinized ES cells were incubated on a gelatinized dish at 37^{o}C for 1h to remove feeders, and 5 x 10^5 cells were split to a non-adherent 6 cm dish and cultured in suspension in ES cell media without leukemia inhibitory factor. After 3-4 days EB were replated on gelatinized

adherent culture dishes for prolonged culture. Gross morphology was examined by staining paraformaldehyde-fixed EB with Giemsa's solution.

Western blot

Whole cell lysate was prepared by dissolving 5 x 10^5 cells in 100 μl of WCL buffer containing 62.5 mM Tris-Cl, 2% SDS, 10% Glycerol, and 5% β-mercaptoethanol. The lysate was then boiled for 10 min and sonicated. After SDS-PAGE and transfer to a nitrocellulose membrane, a western blot was performed with anti-H3K27m3 (#07-449, Upstate Biotechnology, 1:500 dilution) and goat anti-rabbit IgG-HRP (#12-348, Upstate, 1:2000). For reprobing HRP activity was removed by 15% H_2O_2/PBS. The western blot was repeated with anti-Gapdh (#4300, Ambion, 1:1000) and goat anti-mouse IgG-HRP (#12-349, Upstate, 1:2000).

FISH and Immuno-FISH

Xist RNA-FISH was done as described (Lee and Lu, 1999). For immuno-FISH, slides after FISH were post-fixed in 2% paraformaldehyde/PBS and blocked in buffer containing 5% normal goat serum, 0.2% tween20, 0.2% gelatin in 1X PBS(-). Slides were incubated with anti-H4K20m1 (#07-440, Upstate, 1:50) at 4^{o}C overnight, then, incubated in goat anti-rabbit IgG-FITC (AP132F, Chemicon, 1:50) at 37^{o}C for 1 h. Fluorescent microscope images were acquired and adjusted by using the Openlab software (Improvision, Coventry, UK).

Real-time RT-PCR and strand-specific RT-PCR

Total RNA was extracted using Trizol (Invitrogen). For qRT-PCR, total RNA was reverse-transcribed by Superscript III using random primers (Invitrogen). *Xist*, *Tsix* (amplicon 4), *Mecp2*, *Pgk1*, and *Chic1* mRNAs were quantified using TaqMan Universal PCR Master Mix (4324018, Applied

Biosystems) and an ABI Prism 7700 instrument. The results were normalized to *Gapdh* transcript by ΔΔCt method. Pre-designed probes and primers for *Mecp2*, *Pgk1*, *Chic1* and *Gapdh* were purchased from Applied Biosystems (Assay ID Mm00465017_m1, Mm00435617_m1, Mm01232479_m1, and P/N 4308313, respectively), and other probes and primers are shown in Supplementary Table IV. The qRT-PCR amplicon for *Xist* spans an intron and it does not detect *Tsix*. *Tsix* RNA at amplicon 4 (Figure 4D) was quantified in cDNA primed by a gene-specific primer: AAA GGG AAC TTA GAA CAG. *Tsix* RNA at amplicon 5 (Figure 4D), spanning from *Xist* intron 5 to 6 and not detecting transcripts in the *Xist* cDNA Tg, was quantified by using Brilliant II SYBR Green QPCR Master Mix (600828, Stratagene) as described (Shibata and Lee, 2003). All results were from three independent samples or from three independent cell lines (in XY *Eed-TG* and $X^{\Delta}Y$ *Eed-TG* cells). Strand-specific RT-PCR of *Tsix* was as previously described (Stavropoulos *et al*, 2001; Shibata and Lee, 2004). Gene-specific primer and PCR primers for *Gapdh* were: TTG GGT GCA GCG AAC TTT; GCA GTG GCA AAG TGG AGA TTG TTG; CCC TTC CAC AAT GCC AAA GTT GTC. *Gapdh* PCR primers for the SYBR green assay were: GTA GAC AAA ATG GTG AAG GTC GGT; CAA CAA TCT CCA CTT TGC CAC TGC.

Northern blot

Poly-A tailed mRNA was purified using PolyATract mRNA isolation systems (Promega). 2.5 μg of mRNA per lane was run in denaturing 1.2 % agarose gel in 1X MOPS and transferred to a nylon membrane, which was firstly hybridized with random-primed *Mlu*I-*Bsp*MI 0.8 kb fragment (probe 1, Figure 4A), subsequently reprobed with PCR-amplified *Gapdh* 0.4 kb fragment. Sequence integrity of PCR-amplified probe was confirmed.

Methyl-CpG-sensitive Southern blot

Genomic DNA was digested with an excess amount of *Eco*RI, precipitated with ethanol, and dissolved in Tris-EDTA. The DNA concentration was determined and 5 μg of DNA was again digested with *Sac*II or *Hpa*II overnight. Double digested DNA was run in 0.8% agarose gel, transferred, and hybridised with *Mlu*I-*Bsp*MI 0.8 kb fragment at the *Xist* promoter (Figure 5A) or *Bam*HI-*Eco*RI 0.6 kb fragment in exon 1 (Figure 5B).

Quantitative ChIP assay

ChIP assay was done as described (Morshead *et al*, 2003) with little modification. Briefly, fixed cells were aliquoted as 4 x 10^6 cells in a 1.5 ml tube, sonicated by a BIORUPTOR sonicator (Cosmobio, Tokyo, Japan), and incubated with either anti-H3K27m3 (#07-449), anti-H3K4m2 (#07-030, Upstate), or anti-TFIIB (sc-225, Santa Cruz) at 4^{o}C overnight. A mixture of protein A and G sepharose (GE Healthcare) was then added. Immunoprecipitated chromatin DNA was quantified by real-time PCR. Taqman probes and primers were shown in Supplementary Table IV. All results were from three independent samples. Statistical significance of the difference between the results in the XY *Eed-/-* and X$^{\Delta}$Y *Eed-/-* cells was analyzed by student's t-test.

Acknowledgements

We thank M. Asano (Kanazawa Univ.) for the E14.1 cell line, H. Niwa (RIKEN CDB) for the pGT1.8IREShygropA2 plasmid, S. Harada (K.U.) for real-time PCR, and C. Sun (K.U.) for flow cytometry. This work was supported by grants-in-aid from the Ministry of Education, Science, Sports and Culture of Japan (18780250 to S.S.).

References

Azuara V, Perry P, Sauer S, Spivakov M, Jorgensen HF, John RM, Gouti M, Casanova M, Warnes G, Merkenschlager M, Fisher AG (2006) Chromatin signatures of pluripotent cell lines. *Nat Cell Biol* **8:** 532-538

Bacher CP, Guggiari M, Brors B, Augui S, Clerc P, Avner P, Eils R, Heard E (2006) Transient colocalization of X-inactivation centres accompanies the initiation of X inactivation. *Nat Cell Biol* **8:** 293-299

Barr H, Hermann A, Berger J, Tsai HH, Adie K, Prokhortchouk A, Hendrich B, Bird A (2007) Mbd2 contributes to DNA methylation-directed repression of the Xist gene. *Mol Cell Biol* **27:** 3750-3757

Bernstein BE, Mikkelsen TS, Xie X, Kamal M, Huebert DJ, Cuff J, Fry B, Meissner A, Wernig M, Plath K, Jaenisch R, Wagschal A, Feil R, Schreiber SL, Lander ES (2006) A bivalent chromatin structure marks key developmental genes in embryonic stem cells. *Cell* **125:** 315-326

Boyer LA, Plath K, Zeitlinger J, Brambrink T, Medeiros LA, Lee TI, Levine SS, Wernig M, Tajonar A, Ray MK, Bell GW, Otte AP, Vidal M, Gifford DK, Young RA, Jaenisch R (2006) Polycomb complexes repress developmental regulators in murine embryonic stem cells. *Nature* **441:** 349-353

Brockdorff N, Ashworth A, Kay GF, McCabe VM, Norris DP, Cooper PJ, Swift S, Rastan S (1992) The product of the mouse Xist gene is a 15 kb inactive X-specific transcript containing no conserved ORF and located in the nucleus. *Cell* **71:** 515-526

Brown CJ, Hendrich BD, Rupert JL, Lafreniere RG, Xing Y, Lawrence J, Willard HF (1992) The human XIST gene: analysis of a 17 kb inactive X-specific RNA that contains conserved repeats and is highly localized within the nucleus. *Cell* **71:** 527-542

Cao R, Zhang Y (2004) The functions of E(Z)/EZH2-mediated methylation of lysine 27 in histone H3. *Curr Opin Genet Dev* **14:** 155-164

Clemson CM, McNeil JA, Willard HF, Lawrence JB (1996) XIST RNA paints the inactive X chromosome at interphase: evidence for a novel RNA involved in nuclear/chromosome structure. *J Cell Biol* **132:** 259-275

de Napoles M, Mermoud JE, Wakao R, Tang YA, Endoh M, Appanah R, Nesterova TB, Silva J, Otte AP, Vidal M, Koseki H, Brockdorff N (2004) Polycomb group proteins Ring1A/B link ubiquitylation of histone H2A to heritable gene silencing and X inactivation. *Dev Cell* **7**: 663-676

Faust C, Schumacher A, Holdener B, Magnuson T (1995) The eed mutation disrupts anterior mesoderm production in mice. *Development (Cambridge, UK)* **121:** 273-285

Gregory GD, Vakoc CR, Rozovskaia T, Zheng X, Patel S, Nakamura T, Canaani E, Blobel GA (2007) Mammalian ASH1L is a histone methyltransferase that occupies the transcribed region of active genes. *Mol Cell Biol* **27:** 8466-8479

Heard E, Disteche CM (2006) Dosage compensation in mammals: fine-tuning the expression of the X chromosome. *Genes Dev* **20:** 1848-1867

Kalantry S, Magnuson T (2006) The Polycomb group protein EED is dispensable for the initiation of random X-chromosome inactivation. *PLoS Genet* **2:** 656-664

Kalantry S, Mills KC, Yee D, Otte AP, Panning B, Magnuson T (2006) The Polycomb group protein Eed protects the inactive X-chromosome from differentiation-induced reactivation. *Nat Cell Biol* **8:** 195-202

Katayama S, Tomaru Y, Kasukawa T, Waki K, Nakanishi M, Nakamura M, Nishida H, Yap CC, Suzuki M, Kawai J, Suzuki H, Carninci P, Hayashizaki Y, Wells C, Frith M, Ravasi T, Pang KC, Hallinan J, Mattick J, Hume DA et al (2005) Antisense transcription in the mammalian transcriptome. *Science* **309:** 1564-1566

Kohlmaier A, Savarese F, Lachner M, Martens J, Jenuwein T, Wutz A (2004) A chromosomal memory triggered by Xist regulates histone methylation in X inactivation. *PLoS Biol* **2:** 991-1003

Lee JT (2005) Regulation of X-chromosome counting by Tsix and Xite sequences. *Science* **309:** 768-771

Lee JT, Davidow LS, Warshawsky D (1999) Tsix, a gene antisense to Xist at the X-inactivation centre. *Nat Genet* **21:** 400-404

Lee JT, Lu N (1999) Targeted mutagenesis of Tsix leads to nonrandom X inactivation. *Cell* **99:** 47-57

Lee MG, Villa R, Trojer P, Norman J, Yan KP, Reinberg D, Di Croce L, Shiekhattar R (2007) Demethylation of H3K27 regulates polycomb recruitment and H2A ubiquitination. *Science* **318**: 447-450

Luikenhuis S, Wutz A, Jaenisch R (2001) Antisense transcription through the Xist locus mediates Tsix function in embryonic stem cells. *Mol Cell Biol* **21:** 8512-8520

Lyon MF (1961) Gene action in the X-chromosome of the mouse (Mus musculus L.). *Nature* **190:** 372-373

Mager J, Montgomery ND, de Villena FP, Magnuson T (2003) Genome imprinting regulated by the mouse Polycomb group protein Eed. *Nat Genet* **33:** 502-507

Milne TA, Briggs SD, Brock HW, Martin ME, Gibbs D, Allis CD, Hess JL (2002) MLL targets SET domain methyltransferase activity to Hox gene promoters. *Mol Cell* **10:** 1107-1117

Montgomery ND, Yee D, Chen A, Kalantry S, Chamberlain SJ, Otte AP, Magnuson T (2005) The murine polycomb group protein Eed is required for global histone H3 lysine-27 methylation. *Curr Biol* **15:** 942-947

Morey C, Navarro P, Debrand E, Avner P, Rougeulle C, Clerc P (2004) The region 3' to Xist mediates X chromosome counting and H3 Lys-4 dimethylation within the Xist gene. *EMBO J* **23:** 594-604

Morshead KB, Ciccone DN, Taverna SD, Allis CD, Oettinger MA (2003) Antigen receptor loci poised for V(D)J rearrangement are broadly associated with BRG1 and flanked by peaks of histone H3 dimethylated at lysine 4. *Proc Natl Acad Sci USA* **100:** 11577-11582

Navarro P, Page DR, Avner P, Rougeulle C (2006) Tsix-mediated epigenetic switch of a CTCF-flanked region of the Xist promoter determines the Xist transcription program. *Genes Dev* **20:** 2787-2792

Nichols J, Zevnik B, Anastassiadis K, Niwa H, Klewe-Nebenius D, Chambers I, Scholer H, Smith A (1998) Formation of pluripotent stem cells in the mammalian embryo depends on the POU transcription factor Oct4. *Cell* **95:** 379-391

Norris DP, Patel D, Kay GF, Penny GD, Brockdorff N, Sheardown SA, Rastan S (1994) Evidence that random and imprinted Xist expression is controlled by preemptive methylation. *Cell* **77:** 41-51

Ogawa Y, Lee JT (2003) Xite, X-inactivation intergenic transcription elements that regulate the probability of choice. *Mol Cell* **11:** 731-743

Ohhata T, Hoki Y, Sasaki H, Sado T (2006) Tsix-deficient X chromosome does not undergo inactivation in the embryonic lineage in males: implications for Tsix-independent silencing of Xist. *Cytogenet Genome Res* **113:** 345-349

Panning B, Jaenisch R (1996) DNA hypomethylation can activate Xist expression and silence X-linked genes. *Genes Dev* **10:** 1991-2002

Penny GD, Kay GF, Sheardown SA, Rastan S, Brockdorff N (1996) Requirement for Xist in X chromosome inactivation. *Nature* **379:** 131-137

Plath K, Fang J, Mlynarczyk-Evans SK, Cao R, Worringer KA, Wang H, de la Cruz CC, Otte AP, Panning B, Zhang Y (2003) Role of histone H3 lysine 27 methylation in X inactivation. *Science* **300:** 131-135

Sado T, Hoki Y, Sasaki H (2005) Tsix silences Xist through modification of chromatin structure. *Dev Cell* **9:** 159-165

Sado T, Hoki Y, Sasaki H (2006) Tsix defective in splicing is competent to establish Xist silencing. *Development (Cambridge, UK)* **133:** 4925-4931

Sado T, Li E, Sasaki H (2002) Effect of TSIX disruption on XIST expression in male ES cells. *Cytogenet Genome Res* **99:** 115-118

Sado T, Wang Z, Sasaki H, Li E (2001) Regulation of imprinted X-chromosome inactivation in mice by Tsix. *Development (Cambridge, UK)* **128:** 1275-1286

Schoeftner S, Sengupta AK, Kubicek S, Mechtler K, Spahn L, Koseki H, Jenuwein T, Wutz A (2006) Recruitment of PRC1 function at the initiation of X inactivation independent of PRC2 and silencing. *EMBO J* **25:** 3110-3122

Shibata S, Lee JT (2003) Characterization and quantitation of differential Tsix transcripts: implications for Tsix function. *Hum Mol Genet* **12:** 125-136

Shibata S, Lee JT (2004) Tsix transcription- versus RNA-based mechanisms in Xist repression and epigenetic choice. *Curr Biol* **14:** 1747-1754

Shibata S, Yokota T (2008) Alteration of histone tail modifications in the Xist locus in wild-type and Tsix-mutant male embryonic stem cells during differentiation. *Exp Anim* **57:** 153-157

Silva J, Mak W, Zvetkova I, Appanah R, Nesterova TB, Webster Z, Peters AH, Jenuwein T, Otte AP, Brockdorff N (2003) Establishment of histone h3 methylation on the inactive X chromosome requires transient recruitment of Eed-Enx1 polycomb group complexes. *Dev Cell* **4:** 481-495

Smith ER, Lee MG, Winter B, Droz NM, Eissenberg JC, Shiekhattar R, Shilatifard A (2008)

Drosophila UTX is a histone H3 Lys27 demethylase that colocalizes with the elongating form of RNA polymerase II. *Mol Cell Biol* **28**: 1041-1046

Stavropoulos N, Lu N, Lee JT (2001) A functional role for Tsix transcription in blocking Xist RNA accumulation but not in X-chromosome choice. *Proc Natl Acad Sci USA* **98:** 10232-10237

Stock JK, Giadrossi S, Casanova M, Brookes E, Vidal M, Koseki H, Brockdorff N, Fisher AG, Pombo A (2007) Ring1-mediated ubiquitination of H2A restrains poised RNA polymerase II at bivalent genes in mouse ES cells. *Nat Cell Biol* **9**: 1428-1435

Sun BK, Deaton AM, Lee JT (2006) A transient heterochromatic state in Xist preempts X inactivation choice without RNA stabilization. *Mol Cell* **21:** 617-628

Vigneau S, Augui S, Navarro P, Avner P, Clerc P (2006) An essential role for the DXPas34 tandem repeat and Tsix transcription in the counting process of X chromosome inactivation. *Proc Natl Acad Sci USA* **103:** 7390-7395

Wutz A, Jaenisch R (2000) A shift from reversible to irreversible X inactivation is triggered during ES cell differentiation. *Mol Cell* **5:** 695-705

Wutz A, Rasmussen TP, Jaenisch R (2002) Chromosomal silencing and localization are mediated by different domains of Xist RNA. *Nat Genet* **30:** 167-174

Xu N, Tsai CL, Lee JT (2006) Transient homologous chromosome pairing marks the onset of X inactivation. *Science* **311:** 1149-1152

Figure legends

Figure 1. Generation of *Tsix*-trap male ES cells in the *Eed-/-* background ($X^{\Delta}Y$ *Eed-/-*) (**A**) Relationship of ES cell lines generated in this study. *tetOP-Xist*, tetracycline-inducible promoter and *Xist* cDNA (Tg) with *Mus spretus* repeat polymorphism; 11, chromosome 11; X, chromosome X. (**B**) Targeting construct for *Tsix*. Large open and small gray rectangles show *Xist* and *Tsix* exons, respectively. Numbered arrows represent primers for genomic PCR. S, *Spe*I; E, *Eco*RI; B, *Bam*HI restriction enzyme sites. (**C**) *Spe*I-digested Southern blot showing correct recombination of 5'-homology arm in two independent $X^{\Delta}Y$ *Eed-/-* clones. All lanes were derived from the same gel. (**D**) Genomic PCR confirming proper recombination of 3'-homology arm. Primer pair 1-2 was used for mutant (mt) and 1-3 for wild-type (wt) amplification. All lanes were derived from the same gel. (**E**) Rescuing Eed by transfecting the pEGFP-Eed plasmid (XY *Eed-TG* and $X^{\Delta}Y$ *Eed-TG*). Expression of the fusion protein was confirmed by flow cytometry. Results were from the cells at the passage of less than 4 ($X^{\Delta}Y$ *Eed-TG*) or 8 (XY *Eed-TG*) after their derivation. (**F**) Western blot demonstrating reversion of the H3K27m3 modification in the transgenic cell lines. Western blotting was done using cells at the passage of less than 4 ($X^{\Delta}Y$ *Eed-TG*) or 8 (XY *Eed-TG*). Four lanes in the right and left panels were derived from the same gel, respectively.

Figure 2. $X^{\Delta}Y$ *Eed-/-* cells display *Xist* hyperactivation upon differentiation (**A**) *Xist* RNA-FISH using strand-specific riboprobe (red) in the XY *Eed-/-* and (**B**) $X^{\Delta}Y$ *Eed-/-* ES cells differentiated for 3 days. (**C**) The count of *Xist*-positive nuclei in FISH. More than 80 nuclei for the XY *Eed-/-* cell line and more than 180 nuclei for other lines were counted. The $X^{\Delta}Y$ *Eed-/-*1 and $X^{\Delta}Y$ *Eed-/-*2 are independent clones. (**D**) *Xist*

cDNA Tg is inactive in the $X^{\Delta}Y$ *Eed-/-* ES cells, shown by the polymorphism of *Xist* RT-PCR product digested with *Pst*I restriction enzyme. *tetOP-Xist*, *Xist* from the Tg with *Mus spretus* (*M.sp*) sequence. RT-PCR was performed using RNA obtained from the XY *Eed-TG* cells cultured in the presence of doxycyclin for Tg induction. Endo. *Xist*, endogenous *Xist*. RT-PCR in the $X^{\Delta}X$ EB cells in which *Xist* is predominantly expressed from the *Mus musculus* (*M.mus*) allele. $X^{\Delta}Y$ *Eed-/-*, RT-PCR in the $X^{\Delta}Y$ *Eed-/-* EB cells differentiated for 12 days. Shown below is a schematic representation of the PCR products with *M.mus* or *M.sp* repeat polymorphism (open boxes). P, *Pst*I sites. (**E**) Quantitative RT-PCR for *Xist*. Relative amount (mean) of *Xist* RNA to undifferentiated (undif.) wild-type female (XX) ES cells was normalized to *Gapdh* and is shown. Error bars represent SD. (**F**) Rescuing Eed inhibited ectopic *Xist* expression. Relative amount of *Xist* RNA in the $X^{\Delta}Y$ *Eed-/-* day 4 EB to that in the $X^{\Delta}Y$ *Eed-TG* is shown.

Figure 3. Differentiation and XCI of the $X^{\Delta}Y$ *Eed-/-* ES cells

(**A**) Compact colony morphology of the $X^{\Delta}Y$ *Eed-/-* ES cells in undifferentiated condition. (**B**) Morphology of the $X^{\Delta}Y$ *Eed-/-* EB differentiated for 12 days. (**C**) Gross appearance of day 12 EB in the $X^{\Delta}Y$, XY *Eed-/-*, and $X^{\Delta}Y$ *Eed-/-* background. (**D**) Relative amount of X-linked *Mecp2*, *Pgk1* and *Chic1* mRNA in the $X^{\Delta}Y$ *Eed-/-* cells (colored columns) to those in the XY *Eed-/-* cells (gray columns) in undifferentiated or differentiating conditions. Error bars show SD. Asterisks demonstrate statistically significant reduction of the gene expression in the $X^{\Delta}Y$ *Eed-/-* cells (*, $p<0.05$; **, $p<0.0005$). (**E**) Immuno-FISH for H4K20m1 (green) and *Xist* RNA (red) in the $X^{\Delta}X$ and $X^{\Delta}Y$ *Eed-/-* EB (day10-12).

Figure 4. Northern blot and strand-specific or quantitative RT-PCR for *Tsix*

(**A**) Positions of northern blot probe (filled rectangle 1), strand-specific RT-PCR amplicons (2 and 3), and qRT-PCR amplicons (4 and 5). (**B**) Northern blot for *Tsix*. The $X^{\Delta}Y$ *Eed-/-*1 and $X^{\Delta}Y$ *Eed-/-*2, and the $X^{\Delta}Y$ *Eed-TG*1 and $X^{\Delta}Y$ *Eed-TG*2 are independent clones. After the initial northern blot for *Tsix*, the same membrane was stripped and reprobed for *Gapdh*. (**C**) Strand-specific RT-PCR for *Tsix* at the amplicon 2 and 3. (**D**) qRT-PCR for *Tsix* at amplicon 4 and 5. Relative *Tsix* expression levels to the wild-type male (XY) ES cells are shown. Results were from more than three independent samples and error bars indicate SD. Filled circles in the *Tsix* RNA (5) graph represent *Tsix* levels in individual samples of the $X^{\Delta}Y$ *Eed-/-*1 and $X^{\Delta}Y$ *Eed-/-*2 lines.

Figure 5. Methyl-CpG-sensitive Southern blot at the *Xist* promoter and exon 1

(**A**) *Sac*II-digested Southern blot at the *Xist* promoter. Me, methylated; UnMe, unmethylated; E, *Eco*RI site. Position of the probe is shown in the map. Arrow 1, non-specific band found in the XY *Eed-/-* and its derivative lines. (**B**) *Hpa*II-digested Southern blot in the *Xist* exon 1. Arrows 2, 3, and 4 indicate bands originated from *Xist* cDNA Tg. All lanes were derived from the same gel (B), or from twin gels run in parallel (A).

Figure 6. ChIP in male ES cells with mutations in *Eed* and/or *Tsix*

(**A**) Positions of PCR amplicons for ChIP. Those amplicons overlapping with *Xist* cDNA Tg are underlined. ChIP results (mean %IP to input) for (**B**) H3K27m3, (**C**) H3K4m2, and (**D**) TFIIB in undifferentiated condition. (**E**) ChIP for H3K4m2 in day 12 EB. Error bars represent SD. Asterisks in the graphs indicate statistically significant

difference between the XY *Eed-/-* and $X^{\Delta}Y$ *Eed-/-* lines (***, p<0.001; **, p<0.005; *, p<0.05). Differences between other cell lines are not shown for simplicity.

Figure7. Summary of the results and a suggested model

Schematic representation of *Xist* chromatin structure in (**A**) XY (or XY *Eed-TG*), (**B**) $X^{\Delta}Y$ (or $X^{\Delta}Y$ *Eed-TG*), (**C**) XY *Eed-/-*, (**D**) $X^{\Delta}Y$ *Eed-/-* ES cells and (**E**) female future Xi at the onset of XCI. Thick column, *Xist* exon 1; thin column, *Xist* promoter; open lollipops, H3K4m2; filled hexagons, H3K27m3; filled rectangles, methylated CpG. The darkness of the columns represents closed chromatin structure.

Table I The number of nuclei showing colocalization of condensed H4K20m1 and *Xist* RNA in *Xist*-positive nuclei of the mutant EB

Genotype	EB differentiation	H4K20m1 colocalization	No. of *Xist*-positive nuclei counted
$X^{\Delta}X$	7 days	44 (40.4%)	109
$X^{\Delta}Y$ *Eed-/-* 1[*1]	7 days	0 (0%)	142
$X^{\Delta}Y$ *Eed-/-* 1[*1]	18 days	0 (0%)	143
$X^{\Delta}Y$ *Eed-/-* 2[*2]	18 days	0 (0%)	114

[*1] $X^{\Delta}Y$ *Eed-/-* cell clone 1

[*2] $X^{\Delta}Y$ *Eed-/-* cell clone 2

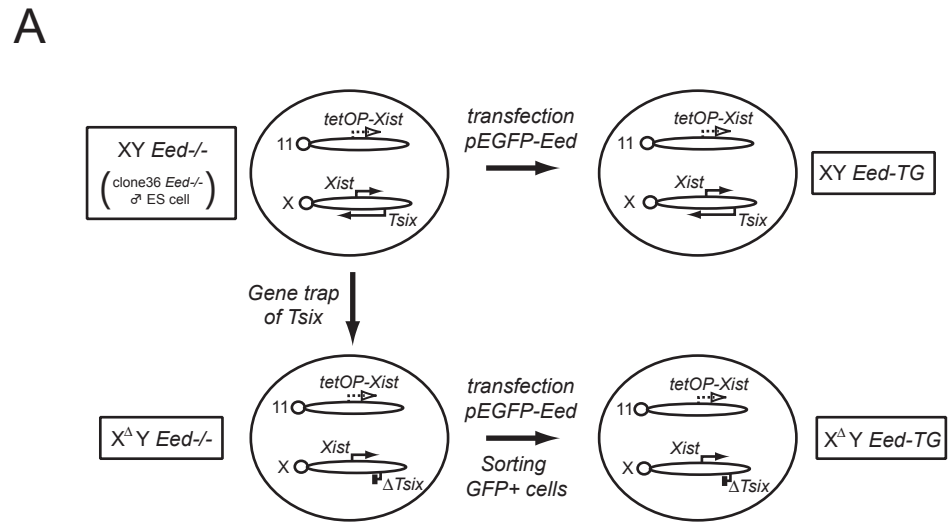

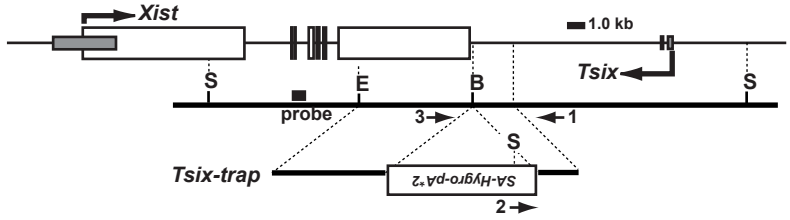

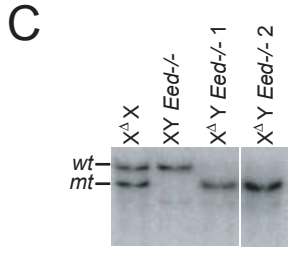

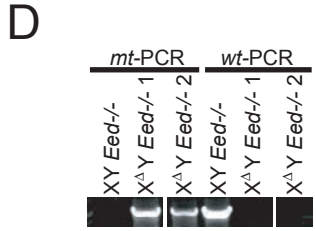

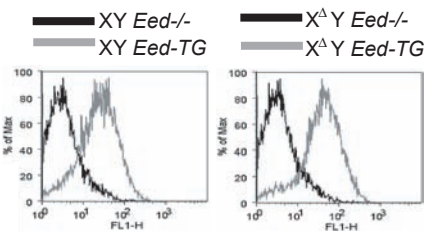

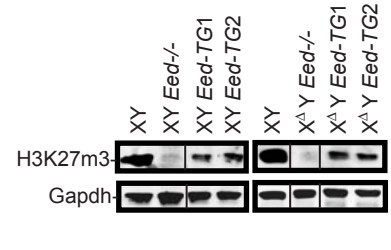

Shibata et al, Figure 1

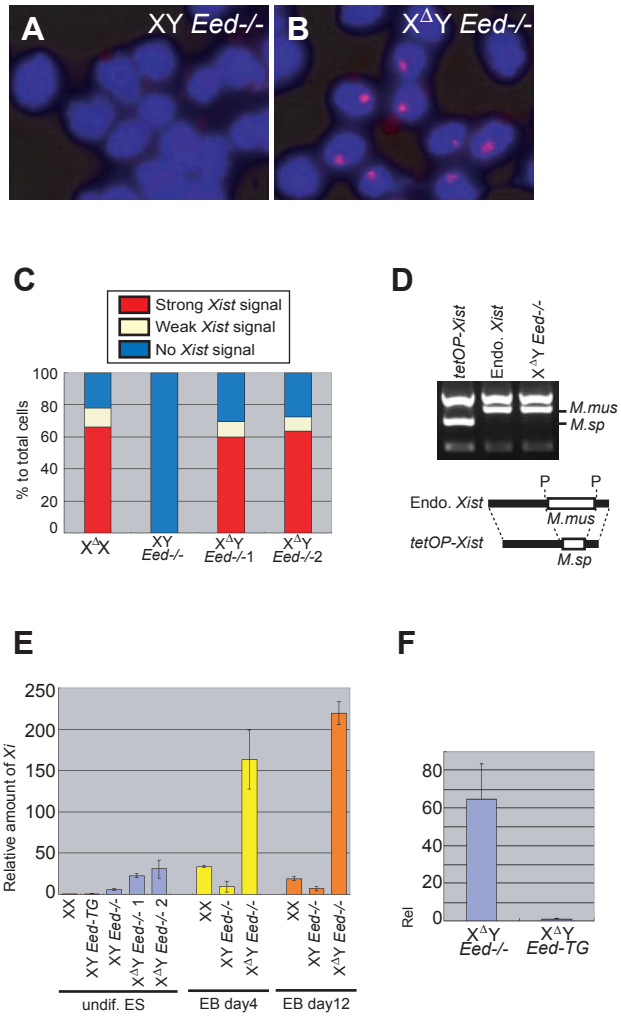

Shibata et al, Figure 2

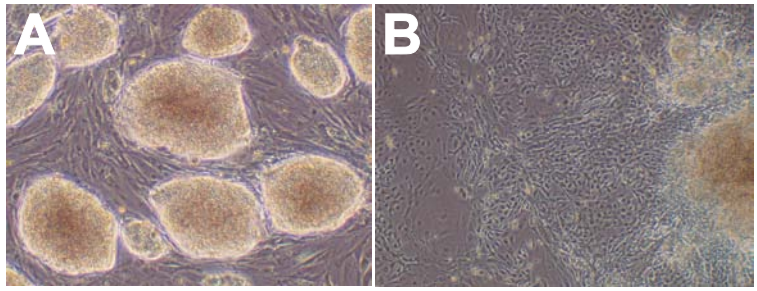

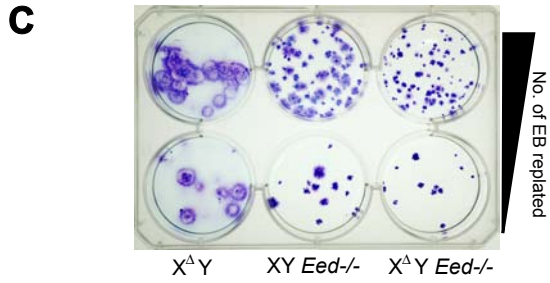

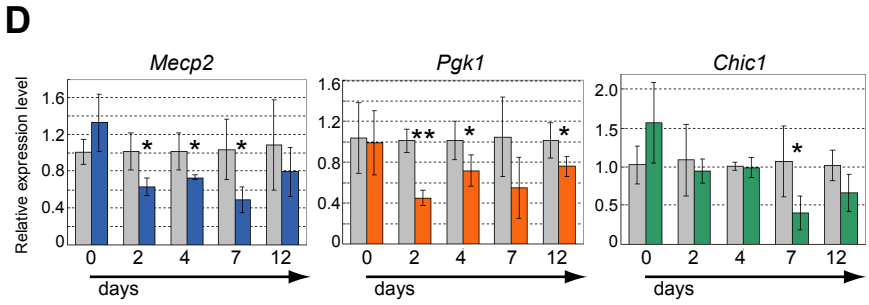

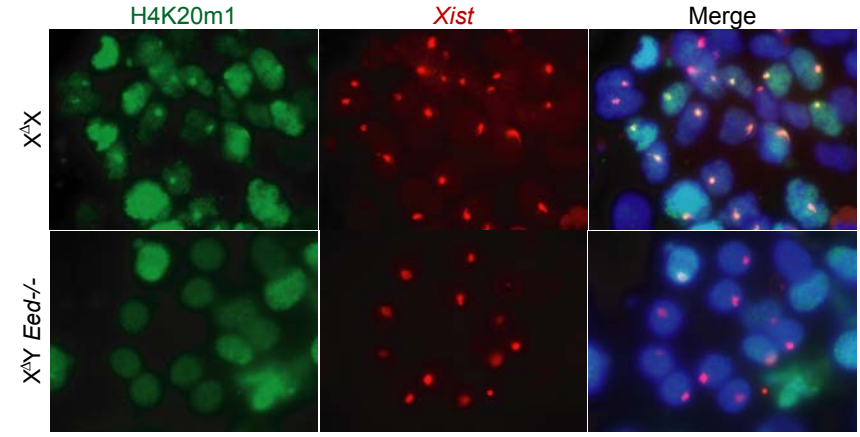

Shibata et al, Figure 3

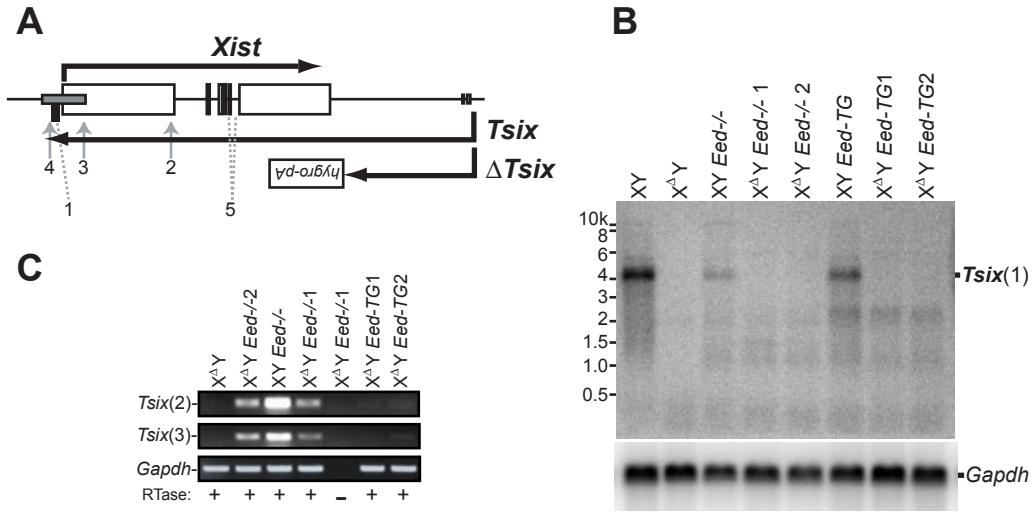

Shibata et al, Figure 4

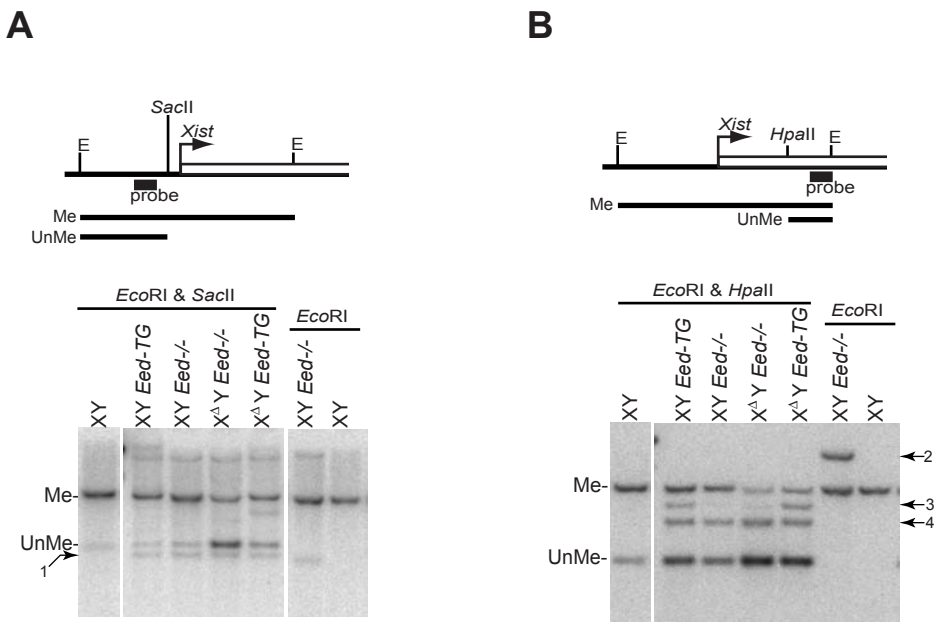

Shibata et al, Figure 5

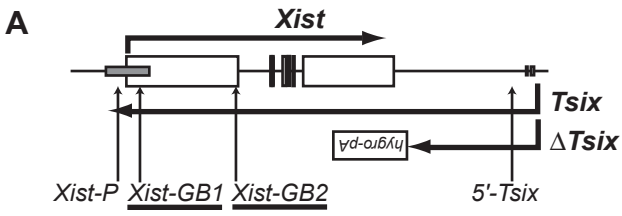

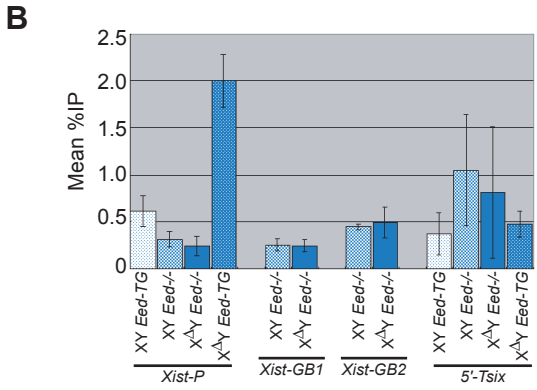

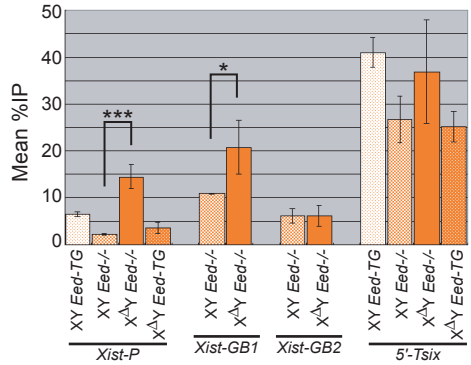

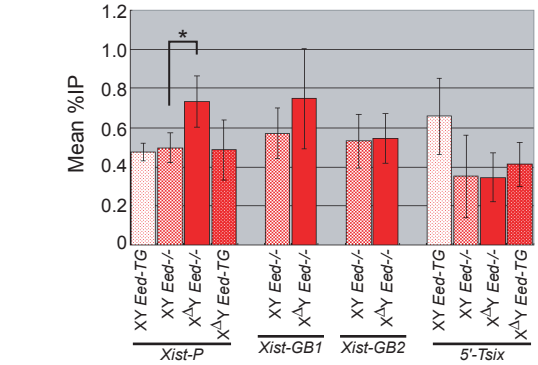

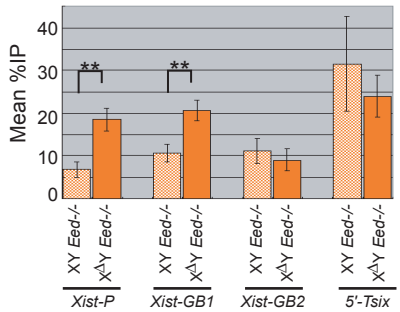

Shibata et al, Figure 6

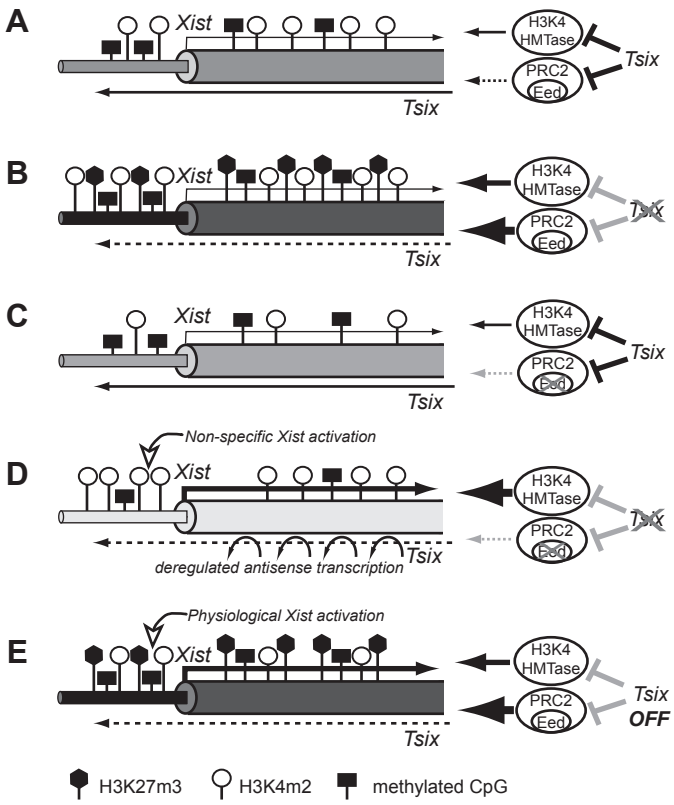

Shibata et al, Figure 7